THE JOURNAL OF BIOLOGICAL CHEMISTRY VOL. 289, NO. 33, pp. 22704–22714, August 15, 2014

Targeting the Ion Channel Kv1.3 with Scorpion Venom Peptides Engineered for Potency, Selectivity, and Half-life

Received for publication, March 25, 2014, and in revised form, June 4, 2014 Published, JBC Papers in Press, June 17, 2014, DOI 10.1074/jbc.M114.568642

Wilson Edwards[1], **Wai-Ping Fung-Leung, Chichi Huang, Ellen Chi, Nancy Wu, Yi Liu, Michael P. Maher, Rachelle Bonesteel, Judith Connor, Ross Fellows, Elena Garcia, Jerry Lee, Lu Lu, Karen Ngo, Brian Scott, Hong Zhou, Ronald V. Swanson, and Alan D. Wickenden**

From Janssen Research and Development, LLC, San Diego, California 92121

Background: The identification of highly selective Kv1.3 blockers has been challenging.
Results: We have engineered scorpion venom peptide fusion proteins to generate potent, selective Kv1.3 inhibitors with long *in vivo* half-lives.
Conclusion: These Kv1.3 inhibitor fusion proteins may have potential for the treatment of autoimmune diseases.
Significance: Our results support an emerging approach to generating subtype selective therapeutic ion channel inhibitors.

Ion channels are an attractive class of drug targets, but progress in developing inhibitors for therapeutic use has been limited largely due to challenges in identifying subtype selective small molecules. Animal venoms provide an alternative source of ion channel modulators, and the venoms of several species, such as scorpions, spiders and snails, are known to be rich sources of ion channel modulating peptides. Importantly, these peptides often bind to hyper-variable extracellular loops, creating the potential for subtype selectivity rarely achieved with small molecules. We have engineered scorpion venom peptides and incorporated them in fusion proteins to generate highly potent and selective Kv1.3 inhibitors with long *in vivo* half-lives. Kv1.3 has been reported to play a role in human T cell activation, and therefore, these Kv1.3 inhibitor fusion proteins may have potential for the treatment of autoimmune diseases. Our results support an emerging approach to generating subtype selective therapeutic ion channel inhibitors.

Ion channels are integral membrane proteins that, through generation of electric currents, regulate diverse cellular functions in excitable tissues such as the heart and central nervous system as well as non-excitable tissue such as lymphocytes, and they are targets for many marketed drugs (1). However, many ion channel drugs are relatively non-selective, often exhibit dose-limiting side effects, and are rarely 100% effective, and there remains a clear need for second generation ion channel drugs with greater selectivity, fewer side effects, and improved efficacy. Unfortunately, the identification of highly selective, second generation, drugs has been challenging, largely due to the fact that the transmembrane regions of ion channels targeted by small molecules are highly conserved among different sub-types (2). With considerable effort failing to yield target selectivity, alternative approaches including the use of new classes of molecules need to be explored. There has been an increasing interest in the use of venom-derived peptides as therapeutics (3, 4). Animal venoms are known to contain a large number of peptides, and many of them target ion channels (5–7). More importantly, these peptides often bind to the poorly conserved extracellular loops of ion channels, offering the potential for significant subtype selectivity. Venom peptides, however, do not usually possess all the necessary properties for successful pharmaceutical development. Their potency and selectivity for the therapeutic target may not be optimal, and their plasma half-lives may not be sufficient for therapeutic applications. These venom peptides, however, may provide suitable starting scaffolds for further modification.

In the present study we focused on the engineering of venom-derived peptides to block Kv1.3, a voltage-gated potassium channel widely recognized as a potential target for the treatment of autoimmune and metabolic diseases (5, 8–18). Members of the α-KTx3 scorpion toxin family, such as OsK1 (α-KTx3.7) and OdK2 (α-KTx3.11), represent promising peptide scaffolds for further engineering. Osk1 and OdK2 are peptides of 38 amino acids in length and are stabilized by three disulfide bonds with paring between Cys-8 and Cys-28, Cys-14 and Cys-33, and Cys-18 and Cys-35 (19, 20). The folded peptides form an α-helix held in close proximity to a three stranded anti-parallel β-sheet by the disulfide bonds. These α-KTx3 like peptides inhibit the voltage-gated potassium channels Kv1.1, Kv1.2, and Kv1.3 through binding to the hypervariable outer vestibule region and occluding the channel pore (21). In this study we showed that OsK1 (19) and OdK2 (20) retained their potassium channel blocking activity when linked to half-life-extending Fc or albumin fusion proteins. We further demonstrated that the potency and selectivity of these fusion proteins on Kv1.3 could be improved through engineering of the peptide and linker regions. Our efforts resulted in the identification of several highly potent, selective, long plasma half-life Kv1.3 blocking fusion proteins that may be useful in the treatment of autoimmune diseases. This approach may also be applicable to targeting other ion channels with therapeutic potential.

EXPERIMENTAL PROCEDURES

Kv Channel Expression Constructs and Cell Lines—Full-length Kv channel cDNA clones, all of human origin unless

[1] To whom correspondence should be addressed: Janssen Research and Development, LLC, 3210 Merryfield Row, San Diego, CA 92121. Tel.: 858-458-3716; E-mail: wedward3@its.jnj.com.

otherwise stated, with accession number in parentheses, were generated using Janssen's GENEWRITER™ proprietary gene assembly technology as previously described (22, 23): Kv1.3 (P22001), Kv1.1 (Q09470), Kv1.2 (P16389), Kv1.5 (P22460), Kv1.6 (P17658), and rat Kv1.3 (rKv1.3) (P15384). Human chimeric channel constructs were generated for higher cell surface expression levels: Kv1.3 E3 chimera was assembled with Kv1.5 amino acids 1–455 and 496–613 and Kv1.3 E3 loop amino acids 456–495; Kv1.1 E3 chimera was assembled with His-tag amino acids 1–9, HRV3C site 10–17, Kv1.5 amino acids 18–472 and 513–630, and Kv1.1 E3 loop amino acids 473–512; Kv1.3 chimera was assembled with Kv1.5 amino acids 1–250 and 497–593 and Kv1.3 amino acids 251–496; Kv1.1 chimera was assembled with Kv1.5 amino acids 1–250 and 492–588 and Kv1.1 amino acids 251–491. Kv channel constructs were cloned into a CMV promoter driven mammalian expression vector and either transiently or stably expressed in HEK or CHO cells. Kv constructs were also cloned into pcDNA4/TO and stably expressed in CHO-TREx cells (Invitrogen) to generate cell lines that expressed human potassium channels in a tetracycline-inducible manner. For electrophysiological experiments, cells were co-transfected with truncated CD4 (pMACs 4.1, Miltenyi Biotech). All cell culture reagents were obtained from Invitrogen. CHO cells transiently expressing Kv1.4, Kv1.6, or Kv1.7 were purchased from Chantest (Cleveland, OH).

Peptide Fusion Protein Expression and Purification—HEK 293-E cells were transfected with plasmid DNA using Lipofectamine 2000 (Invitrogen) or Max transfection reagent. Peptide-Fc fusion proteins were purified from day 4 culture supernatants using Protein A-Sepharose 4FF resin or an AKTA XpressTM chromatography system (GE Healthcare). His-tagged peptide fusions were purified on a HisTrap column. Protein concentrations were determined by absorbance at 280 and 310 nm on a BioTek SynergyHTTM spectrophotometer. If necessary, the purified proteins were concentrated with a 10,000 molecular weight cutoff centrifugal concentrator (Millipore). The quality of the purified proteins was assessed by SDS-PAGE and analytical size exclusion HPLC (Dionex HPLC system). Endotoxin levels were measured using a limulus amebocyte lysate (LAL) assay.

Synthesis of KV261 Peptide—Peptide synthesis was performed on Fmoc-Lys(Boc)-Wang (Boc, *t*-butoxycarbonyl) resin 0.47 mmol/g substitution (Peptides International) via solid phase peptide synthesis (SPPS) using an ABI Model 433A automated peptide synthesizer. The standard 0.1-mmol-scale FastMoc MonPrevPeak protocols were used for HBTU/HOBt/DIEA (*N,N*-diisopropylethylamine/2-(1*H*-benzotriazole-1-yl)-1,1,3,3-tetramethyluronium hexafluorophosphate/hydroxybenzotriazole) activation. Pseudoproline dipeptide Fmoc-Ile-Ser(ΨMeMepro)-OH (Fmoc, *N*-(9-fluorenyl)methoxycarbonyl; Novabiochem) was incorporated at the position shown in bold and underlined in the sequence GVPINVKC-K**IS**RQCIEPCKDAGMRFGKCMNGKCHCTPK resin. The amino acid side-chain functionality was protected as follows: Arg(Pmc), Asn(Trt), Asp(OtBu), Cys(Trt), Glu(OtBu), Gln(Trt), Lys(Boc), Ser(tBu), and Thr(tBu) (Boc, *t*-butoxycarbonyl) (where Pmc is 2,2,5,7,8-pentamethyl-chroman-6-sulfonyl chloride and Trt is triphenylmethyl). Peptide was cleaved from the resin with TFA buffer (1.5 g of phenol in 4 ml of 1,2 ethanedithiol, 1 ml of thioanisole, 1 ml of water, and 1 ml of triisopropylsilane) and precipitated with precooled ethyl ether. The peptide was oxidized at 100 μg/ml in 0.1 M Tris-HCL, 1 M guanidine-HCL, 1 mM EDTA, 3 mM reduced glutathione, and 0.3 mM oxidized glutathione, and the reaction was stopped by reducing the pH to 3.9 with glacial acetic acid. The peptide was lyophilized, purified by Vydac C-18 RP-HPLC, and analyzed with RP-HPLC, capillary electrophoresis, and LC/MC on purity and molecular mass.

Direct Binding Assays—HEK 293F cells (Invitrogen) stably transfected with chimeric Kv channel expression constructs were cultured in DMEM supplemented with 10% FBS and 600 μg/ml Geneticin (all reagents from Invitrogen). Kv-transfected cells at 2×10^5 cells/well in 96-well V bottom polypropylene plates (Costar) were treated with venom peptide fusion samples in spent Freestyle 293 media or in PBS supplemented with 2% FBS (FACS buffer) at 4 °C for 1 h. Cells were then washed with FACS buffer and incubated with either Cy5-conjugated goat anti-human Fc Fab′2 (Jackson ImmunoResearch Inc.) or a 1:200 mixture of biotinylated goat anti-human albumin (Abcam) and streptavidin-phycoerythrin. Cells after staining were washed with FACS buffer, fixed with Cytofix™ fixation buffer (BD Biosciences), and acquired with the FACSArray flow cytometer (BD Biosciences). Data were analyzed in FlowJo software (Treestar), and geometric mean fluorescence intensities of cell-bound peptide fusions were compared with Odk2-Fc or KV261-HSA-23 and reported as % parent.

Competitive Binding Assay—Binding of peptides or peptide fusion proteins to cells transfected with chimeric Kv1.3 was performed as described in the previous section followed by 1 h of incubation with agitoxin-2-Cys-6-carboxytetramethylrhodamine (10 nM, Alomone). Cells were then washed with FACS buffer and acquired for analysis as described in the previous section. For K_i calculations, the K_D value for agitoxin-2-Cys-6-carboxytetramethylrhodamine was determined to be 0.2 nM by whole cell manual patch-clamp electrophysiology (data not shown; see also Ref. 24).

T Cell Activation Assay—Human $CD4^+$ T cells (AllCells LLC) were cultured in RPMI 1640 medium (Invitrogen) supplemented with 1% normal human A/B serum (Valley Biomedical Products & Service Inc.) at 2×10^5 cells/well in 96-well flat-bottom culture plates (NUNC). Cell culture media was supplemented with 2% HSA[2] (Sigma) for testing HSA fusions. $CD4^+$ T cells were pretreated with Kv1.3 blockers and controls for 30 min before overnight stimulation with human T cell expansion beads (Miltenyi Biotec) at a 1:1 bead to cell ratio. IL-2 levels in supernatants were measured with a chemiluminescent immunoassay derived from the human IL-2 Quantikine Kit (R&D Systems).

Human Peripheral Blood Mononuclear Cell (PBMC) Cytokine Induction Assay—Human PBMCs were obtained from AllCells LLC or purified from healthy donor blood by Ficoll-Paque

[2] The abbreviations used are: HSA, human serum albumin; KLH, keyhole limpet hemocyanin; DTH, delayed-type hypersensitivity; PBMC, peripheral blood mononuclear cell; Fmoc, *N*-(9-fluorenyl)methoxycarbonyl.

(GE Healthcare) density centrifugation. Purified PBMCs were plated in 96-well culture plates at 1×10^6 cells/well in RPMI medium supplemented with 10% FBS and incubated overnight with Kv1.3 blockers. Cytokines in overnight PBMC culture supernatants were detected with TH1/TH2 10-plex human cytokine kit (Meso Scale Discovery).

Electrophysiology—Cells for use in electrophysiological assays were plated at low density onto glass coverslips 24 h before recording and maintained in appropriate media. On the day of the experiment, glass coverslips were placed in a bath on the stage of an inverted microscope and perfused (~1 ml/min) with an extracellular solution of the following composition: 137 mM NaCl, 2 mM $CaCl_2$, 5.4 mM KCl, 1 mM $MgCl_2$, 5 mM glucose, 10 mM HEPES, and 0.1% bovine serum albumin, pH 7.4. Pipettes were filled with an intracellular solution of the following composition: 40 mM KCl, 100 mM KF, 2 mM $MgCl_2$, 10 mM EGTA, 10 mM HEPES, pH 7.3 to 7.4, and had a resistance of 2–4 megaohms. All recordings were made at room temperature (22–24 °C) using a Multiclamp 700A amplifier and pClamp 9 software (Axon Instruments). Transiently transfected CHO cells were identified using anti-CD4-coated beads (Dynabeads, Invitrogen). Outward potassium currents were measured using the whole-cell configuration of the patch clamp technique at a test potential of 20–40 mV from a holding potential of −80 mV. Current records were acquired at 2–5 KHz and filtered at 1–2 KHz. Uncompensated series resistance was typically <10 megaohms, and 80% series resistance compensation was routinely applied. Currents were elicited once every 20s and were allowed to stabilize for 5–10 min before recording. Compounds were applied using an SF-77B Fast-Step Perfusion device (Warner Instruments). 1–4 concentrations of compound were tested per cell.

Thallium Flux—Chimeric Kv channel expressing HEK293F cells were plated at 10,000 cells per well into poly-lysine-coated 384-well microtiter plates (BD Biosciences). Cell plates were washed with assay buffer (130 mM NaCl, 4 mM KCl, 2 mM $CaCl_2$, 1 mM $MgCl_2$, 10 mM HEPES, 5 mM glucose) using a Biotek EL405. Cells were stained for 30 min with FluxOR dye (Invitrogen) in assay buffer plus 2 mM probenecid at room temperature in the dark. The dye was then washed off with assay buffer. Thallium dye fluorescence in response to the addition of stimulus buffer was monitored in the presence or absence of test compounds using a FLIPR Tetra (Molecular Devices). The stimulus buffer contained 180 mM HEPES, 90 mM KOH, 2 mM $CaCl_2$, 1 mM $MgCl_2$, 5 mM glucose, 1 mM Tl_2SO_4. The fluorescence change was measured 20 s after adding the stimulation buffer. Data were normalized to the average responses of control wells ($n = 16$ each of 10 nM *Stichodactyla* toxin peptide (ShK) for full inhibition controls and buffer-only for zero inhibition controls).

Determination of Fusion Proteins in Plasma—Controls and standards were prepared in normal plasma (Bioreclamation). Concentrations of intact peptide-Fc fusion proteins in plasma were determined using direct binding assays as described above.

The Fc portion of fusion proteins in plasma was detected by ELISA. Goat anti-human Fc polyclonal capture antibody (Jackson ImmunoResearch Inc.) was immobilized onto 96-well plates (Nunc), and HRP-conjugated donkey anti-human Fc polyclonal antibody (Jackson ImmunoResearch Inc.) was used to detect the captured Fc proteins using BM chemiluminescent substrate (Roche Applied Science) and an Envision plate reader (PerkinElmer Life Sciences).

Plasma concentrations of HSA, KV261 peptide, or KV261-HSA fusions were also measured in chemiluminescent ELISA assays. KV261 in plasma was measured using 384-well plates (Nunc) coated with anti-KV261 rabbit polyclonal capture antibody and detected with a 1:1000 mixture of biotinylated rabbit anti-261peptide polyclonal antibody and HRP-conjugated streptavidin (Roche Applied Science). HSA in plasma was measured using 384-well streptavidin-coated plates (Nunc) with biotinylated mouse anti-human albumin monoclonal capture antibody (Abcam) and detected with HRP-conjugated sheep anti-human albumin polyclonal antibody (Abcam). Minipig plasma samples used HRP-conjugated anti-penta-His (Qiagen) to detect the His tag on the C terminus of the fusion protein. All assays used chemiluminescent substrate (Roche Applied Science) and an Envision plate reader (PerkinElmer Life Sciences).

In Vitro Thapsigargin-stimulated IL-17A Production from Whole Blood—Heparinized blood from Yucatan swine or human donors was diluted with an equal volume of IMDM medium supplemented with 2% normal human A/B serum (Valley Biomedical Products & Service Inc.) and stimulated with 10 μM thapsigargin (Alomone) for 20 h. IL-17A levels in culture supernatants were measured in electrochemiluminescent immunoassays using a MA6000 plate reader (Meso Scale Discovery). Pig IL-17A was captured and detected with specific antibodies (Bethyl Laboratories), and purified porcine IL-17A was used as a standard. Human IL-17A was detected with an IL-17A MSD kit (Meso Scale Discovery). Measurement of IL-17A blocking effects by peptides, fusion proteins, or cyclosporine A was performed by preincubation of blood with compounds for 1 h before thapsigargin stimulation.

Pharmacokinetic Studies—Pharmacokinetic studies in rats were performed at the animal facility of Janssen R&D, San Diego, and the animal work was approved by the Institutional Animal Care and Use Committee of Janssen R&D. Sprague-Dawley rats were dosed with KV261-Fc (3.0 mg/Kg) or KV261-HSA-34 (2.3 mg/Kg) by intravenous bolus, and blood samples were collected at time points up to 4 days. Compound plasma levels were analyzed in ELISA- and FACS-based assays to detect specifically the intact fusion proteins, the fusion partners, and the KV261 peptide as described in previous sections.

Animal work on minipigs was performed by Comparative Biosciences, Inc. (Sunnyvale, CA) and approved by the Institutional Animal Care and Use Committee of Comparative Biosciences. Pharmacokinetics of KV261-HSA-34 in Yucatan minipigs was tested after intravenous administration of the fusion protein at 2.3 mg/Kg, and blood samples were collected at time points up to day 56. KV261-HSA-34 plasma levels were measured in ELISA assays to specifically detect the intact fusion protein, the fusion partner, and the KV261 peptide as described in previous sections. Pharmacokinetic parameters were calculated using Phoenix WinNonlin pharmacokinetic modeling software program (Certara).

Ex Vivo Thapsigargin-stimulated IL-17A Production from Minipig Whole Blood—Heparinized blood (3 ml/animal) was collected from minipigs either untreated ($n = 1$) or injected with fusion protein ($n = 4$). Each blood sample was treated with 10 μM thapsigargin alone or thapsigargin plus 1 μM KV261. IL-17A concentrations were measured as described above. Inhibition of IL-17A production by exogenous KV261 was calculated as follows.

$$\%\ \text{Inhibition by exogenous KV261} = ((\text{thapsigargin (IL-17A)} - \text{thapsigargin} + 1\ \mu\text{M KV261 (IL-17A)}/\text{thapsigargin (IL-17A)}))\times 100 \quad \text{(Eq. 1)}$$

A low % inhibition by exogenous KV261 for a given sample indicated all or the majority of Kv1.3-dependent IL-17A production was blocked by the injected fusion protein and was evidence of target engagement.

Minipig Delayed-type Hypersensitivity Model—Female Yucatan miniature swine, *Sus scrofa domestica* (Sinclair BioResources, LLC; Columbia, MO), at 3–7 months old weighing 12–35 kg were used in delayed-type hypersensitivity (DTH) studies. Studies were performed by Comparative Biosciences and were approved by the Institutional Animal Care and Use Committee of Comparative Biosciences. Keyhole limpet hemocyanin (KLH) (Sigma) at 10 mg/ml was emulsified with incomplete Freund's adjuvant (BD Biosciences) at a 1:1 volume ratio. On day 0 animals were immunized by subcutaneous injection of 1 ml of KLH/incomplete Freund's adjuvant emulsion per site at ~5 sites on the caudal aspect of the hind legs. Unimmunized control pigs were injected with PBS/incomplete Freund's adjuvant emulsion following the same procedures. On day 7, all animals were challenged by intradermal injection on the flanks with KLH at 10, 5, 2.5, and 1.25 mg/ml and PBS negative control, 0.1 ml per injection, and 2 injections per dose level. KV261-HSA-34 at 2.3 mg/ml and PBS vehicle control were dosed intravenously in a blinded fashion at 1 ml/kg on day −1 and day 6. Cyclosporine A, an immune suppressant known to be effective in DTH and transplantation models in rodents and minipigs (25–27), was used as a positive control. Cyclosporine A (Sandimmune) was dosed subcutaneously at 10 mg/ml and 1 ml/kg, twice daily from day −1 through day 8. The dosing regimens of KV261-HSA-34 and cyclosporine A used in this study blocked thapsigargin-induced IL-17A in minipig blood in preliminary experiments (data not shown). Induration at the challenge sites was measured at day 6 before antigen challenge and 1 and 2 days after challenge. Blood was collected at preimmunization and at 2 days post challenge for pharmacodynamic and bioanalytical tests. Necropsy was performed 2 days after the challenge. Skin biopsies at the challenge sites, draining inguinal nodes, and blood samples were collected at necropsy. Skin biopsies were fixed and stained with hematoxylin and eosin (H&E) for histopathology evaluation. Skin sections were examined microscopically to assess inflammation scores based on the extent of inflammatory cell infiltration as well as ulceration and hyperkeratosis at the epidermis. Single cell suspensions were prepared from draining inguinal nodes, and cell numbers were counted with a hemocytometer. KLH-specific antibody titers in plasma were measured with ELISA.

Data Analysis and Statistics—Values are reported as the means ± S.E. of the mean. Concentration-response data were fitted by non-linear regression (Graph Pad Prism, Version 4.0) using a four-parameter general logistic equation.

Student's *t* test was performed on results from the draining lymph node cellularity data using PRISM (GraphPad). Concentrations of unknowns from quantitative immunoassays were determined from regression analysis of acquired raw data performed using SoftMaxPro (Molecular Devices).

Materials—The OdK2 scorpion peptide extracted from the venom of *Odontobuthus doriae* was provided by Professor Jan Tytgat, Laboratory of Toxicology, University of Leuven (KU Leuven). Recombinant OsK1 peptide was obtained from Alomone Labs (Jerusalem, Israel).

RESULTS

Generation of Kv1.3 Blocking Scorpion Peptide Fc Fusion Proteins—To determine if the potassium channel blocking activity of OsK1 and Odk2 venom peptides could be retained as Fc fusion proteins, the C terminus of each peptide was fused to the Fc fragment of a human IgG4 antibody via a $GS(G_4S)_4$ linker (Fig. 1*a*). These fusion proteins formed dimers through the Fc region, resulting in a bivalent display of the respective peptides. Potency of OdK2-Fc and OsK1-Fc in blocking potassium channels was evaluated in manual patch clamp studies, and representative recordings of Kv1.3 currents in transfected CHO cells treated with OdK2-Fc are shown (Fig. 1*b*). Both OdK2-Fc and OsK1-Fc were active in blocking Kv1.3 with IC_{50} values of 15.5 ± 5.1 and 0.31 ± 0.02 nM respectively. However, their potencies were ~15–150-fold less potent than the peptides (Table 1). Further characterization of the fusion proteins revealed that OdK2-Fc had improved selectivity, with 56-fold selectivity for Kv1.3 over Kv1.1 and no cross-reactivity with Kv1.2 at concentrations up to 1 μM. Osk1-Fc was 8-fold selective for Kv1.3 over Kv1.1. Kv1.3 has been suggested to play a role in modulating T cell activation (28, 29). We, therefore, assessed the inhibitory effects of venom peptide-Fc fusions on IL-2 production from anti-CD3- and anti-CD28-stimulated primary human $CD4^+$ T cells. OdK2-Fc, OsK1-Fc, and OsK1 peptide were effective in blocking IL-2 production from activated T cells (Fig. 1, *c*, *d*, and *g*). Similar to the findings in Kv1.3 electrophysiology, the potency of OsK1-Fc fusion was reduced compared with the free peptide. These data demonstrate that fusions of human IgG4 Fc with OdK2 and OsK1 peptides are functional in blocking Kv1.3 currents as well as inhibiting T cell activation, albeit with reduced potency.

Peptide Engineering to Improve Potency and Selectivity—To generate Fc fusions with the high potency of OsK1-Fc and the greater selectivity of OdK2-Fc, we prepared a combinatorial library of peptide-Fc variants with the peptide regions variegated to create OdK2 and OsK1 chimeras at eight of the nine positions that are divergent between OdK2 and OsK1. The library design interchanged OdK2 and OsK1 amino acids at positions 3, 4, 5, 9, 10, 12, 16, and 20 in a fully combinatorial manner. Isoleucine and leucine at position 15 were not included due to the similarity of these two amino acids. This library also included the incorporation of lysine at position 16 in some of the variants, as this mutation has been shown to

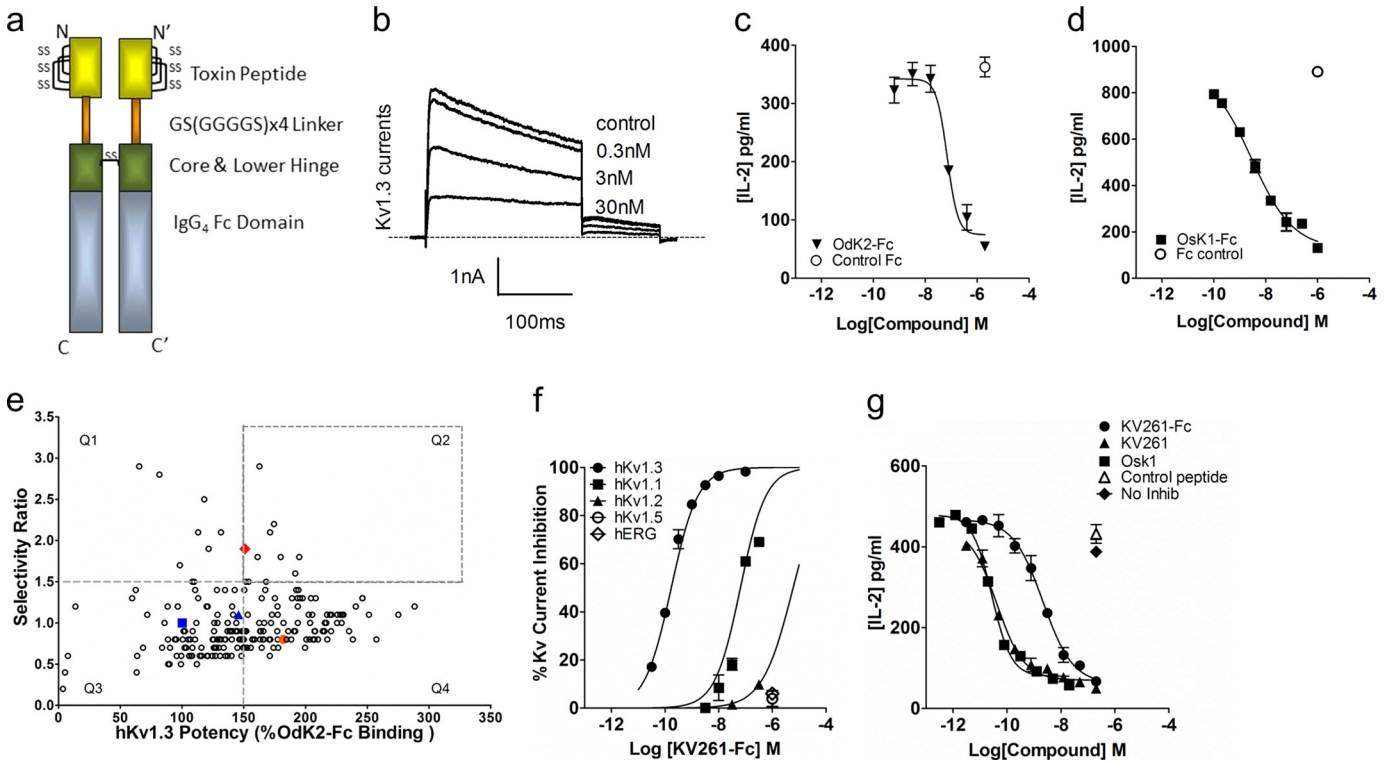

FIGURE 1. **Toxin peptide Fc fusion proteins are active, can be engineered for potency and selectivity, and inhibit *in vitro* human T cell activation.** *a*, schematic representation of a toxin peptide-Fc fusion protein showing the Fc from a human IgG4 fused with the peptide C terminus with an intervening $(G_4S)_4$ linker. The peptide-Fc molecule is a covalent dimer with disulfide bonds (*SS*) between the adjoining core/lower hinge regions. The *upper hinge region* was removed from the Fc region for design of these fusions. The *N* and *C* designate the termini for Fc1 and N′ and C′ for Fc2 of the dimer, with predicted disulfide bonds designated (*SS*). *b*, OdK2-Fc fusion protein inhibits human Kv1.3 whole cell currents in a concentration-dependent manner in transfected CHO cells. *c* and *d*, inhibition of IL-2 production from anti-CD3/anti-CD28-stimulated human $CD4^+$ T cells by OdK2-Fc and Osk1-Fc. *e*, primary screening results of chimera library variants (○) showing the relationship between Kv1.3 potency (% OdK2-Fc binding) and selectivity (binding ratio of Kv1.3/Kv1.1). OdK2-Fc parent control (■), OdK2-Fc parent recurrent in the library (▲), OsK1-Fc parent control (●), and lead variant KV1261-Fc (♦) are highlighted. Hits demonstrating improved selectivity as well as high Kv1.3 potency relative to OdK2-Fc are located in quadrant 2 (*Q2*). *f*, inhibition of Kv channels and hERG by KV261-Fc. These results indicate that the fusion protein is highly selective for Kv1.3. *g*, inhibition of IL-2 production from anti-CD3/anti-CD28-stimulated human $CD4^+$ T cells by Osk1, KV261, and KV261-Fc.

increase the potency of OsK1 on Kv1.3 (19). This resulted in a total number of 262 library variants. The library was expressed in crude supernatants from HEK cells transfected with individual library clones and screened for binding to cells expressing Kv1.3 or Kv1.1 relative to the parent OdK2-Fc (Fig. 1*e*). In Fig. 1*e*, peptide-Fc variants on the *right of the vertical intersection* show better binding to Kv1.3 (>150% of OdK2-Fc binding), and those *above the horizontal intersection* have better Kv1.3 selectivity (>1.5 fold better than OdK2-Fc). Variants with improved potency and selectivity on Kv1.3 are located in quadrant 2 (*Q2*). Several promising variant clones were identified, all of which had proline at position 3, isoleucine at position 10, and glutamic acid at position 16 (Fig. 1*e*, Table 1). None of these variants contained lysine at position 16. Variant KV261-Fc possessed the best potency and selectivity profile, with an IC_{50} of 0.15 ± 0.01 nM on Kv1.3 and selectivity of 710-fold over Kv1.1 (IC_{50} of 106.6 ± 21.9 nM) and >2000-fold over Kv1.2 (IC_{50} > 300 nM), Kv1.5 (IC_{50} > 1 μM), and Kv11.1, hERG, channel (IC_{50} > 1 μM) (Table 1, Fig. 1*f*). KV261-Fc was also efficacious in inhibiting IL-2 production from anti-CD3- and anti-CD28-stimulated human $CD4^+$ T cells with an IC_{50} of 3.2 ± 0.7 nM (Fig. 1*g*). Potency of KV261-Fc was similar to OsK1-Fc in both electrophysiology and T cell assays, whereas its target selectivity was higher than OsK1-Fc and OdK2-Fc (Table 1). A synthetic version of the KV261-Fc peptide region, KV261, was shown to be highly potent on Kv1.3 with an IC_{50} of 0.019 ± 0.003 nM and selective over Kv1.1 (IC_{50} of 3.4 ± 1.0 nM) (Table 1) and Kv1.2 (IC_{50} of 69.1 ± 9.0 nM). KV261 peptide also potently inhibited IL-2 production from activated human $CD4^+$ T cells (IC_{50} of 0.05 ± 0.01 nM) (Fig. 1*g*). The results suggest that the engineered peptide region as represented by KV261 contributes to the selectivity and potency of KV261-Fc.

During exploration of Kv1.3 biology in human PBMCs we observed Kv1.3 blocking peptide-Fc fusions caused an induction of inflammatory cytokines from PBMCs (Table 2). This effect was seen with all peptide Fc fusions tested including OdK2-Fc, OsK1-Fc, and ShK-Fc (data not shown). Induced cytokine release was not observed with peptides or with Fc controls. Based on these findings it appeared that inflammatory cytokines released from human PBMCs could result from either bivalent peptide display, Fc effector function, or a combination of these features. We reasoned, therefore, that monovalent non-Fc peptide fusions might avert this potentially deleterious property.

Monovalent Peptide Fusion with Human Serum Albumin—Monovalent non-Fc fusion proteins were generated with HSA as the fusion partner (Fig. 2*a*). Fusions of HSA to the N terminus of the KV261 peptide had no detectable activity (data not

TABLE 1

Summary of the sequence and activity of chimera library-Fc fusion variants

The potency and selectivity of chimera library-Fc fusion variants for Kv1.3 over Kv1.1 are shown. These variants include KV261-Fc and the parents OdK2-Fc and OsK1-Fc as well as their corresponding free peptides. The amino acid sequences of OdK2 and OsK1 peptides are aligned with disparate amino acids highlighted in gray. The variegated sequence of each variant with the change and position in amino acids are also indicated.

```
          1                   10                  20                  30
OdK2      G V P T D V K C R G S P Q C I Q P C K D A G M R F G K C M N G K C H C T P K
OsK1      G V I I N V K C K I S R Q C L E P C K K A G M R F G K C M N G K C H C T P K
```

Compound ID	Kv1.3 IC_{50} (nM) ± S.E.	Kv1.1 IC_{50} (nM) ± S.E.	Fold Selectivity	Variegated Position								
				3	4	5	9	10	12	15	16	20
KV261-Fc	0.15 ± 0.011	106.60 ± 21.9	710	P	I	N	K	I	R	I	E	D
KV261	0.02 ± 0.003	3.40 ± 1.0	170	P	I	N	K	I	R	I	E	D
KV197-Fc	0.39 ± 0.100	200.90 ± 88.3	515	P	I	D	K	I	R	I	E	D
KV37-Fc	0.48 ± 0.110	156.30 ± 15.6	326	P	T	D	R	I	R	I	E	D
KV229-Fc	0.27 ± 0.070	100.50 ± 56.3	372	P	T	N	K	I	R	I	E	D
KV267-Fc	0.38 ± 0.150	105.40 ± 22.3	277	P	I	N	K	I	P	I	E	K
OdK2-Fc	15.50 ± 5.100	871.60 ± 271.0	56	P	T	D	R	G	P	I	Q	D
OdK2	0.10 ± 0.010	1.89 ± 0.2	18	P	T	D	R	G	P	I	Q	D
OsK1-Fc	0.31 ± 0.020	2.50 ± 0.5	8	I	I	N	K	I	R	L	E	K
OsK1	0.02 ± 0.004	0.22 ± 0.1	12	I	I	N	K	I	R	L	E	K

TABLE 2

Induction of inflammatory cytokines from PBMCs by KV261-Fc fusion protein

Inflammatory cytokines IFNγ, IL-1β, and TNFα were measured in human PBMC cultures after overnight treatment with various Kv1.3 blockers (all 2 μM) including KV261-Fc, KV261-HSA-34, KV261-HSA-686, and KV261 and controls including IgG4 Fc and HSA and no treatment. Cytokine measurements were performed as described under "Experimental Procedures," and values are shown as averages of duplicates ± S.E. Values of <10.0 indicate cytokine levels were below the 10 pg/ml limit of detection.

Blocker ID	Description	Cytokines (pg/ml)		
		IFNγ	IL-1β	TNFα
KV261-Fc	261-$GS(G_4S)_4$-Fc	236.3 ± 35.4	7202.6 ± 432.7	11104.8 ± 304.3
KV261-HSA-34	261-$AS(AP)_{20}$GS-HSA	<10.0	33.5 ± 22.4	57.4 ± 41.7
KV261-HSA-686	261-AHRH-$AS(AP)_{20}$GS-HSA	<10.0	71 ± 1.3	169 ± 38.4
KV261	261 peptide	<10.0	26.9 ± 1.6	41.7 ± 2.8
IgG4 Fc	Recombinant human Fc	<10.0	44.9 ± 1.3	140.8 ± 35.6
HSA	Recombinant human albumin	<10.0	71.8 ± 22.4	144 ± 10.3
No treatment	Buffer	<10.0	42.1 ± 0.4	144.4 ± 27.2

shown). KV261-HSA-23 had HSA fused to the C terminus of KV261 via a $GS(G_4S)_4$ linker and was active but with considerably lower potency compared with the KV261 peptide and KV261-Fc. KV261-HSA-23 inhibited Kv1.3 currents and IL-2 production from activated human $CD4^+$ T cells with IC_{50} values of 14.7 ± 0.7 nM (Fig. 2*i*) and 47.7 ± 5.1 nM (Fig. 2*b*), respectively. The reduced potency relative to the Fc fusion may partly be explained by the reduced avidity as a monovalent fusion protein. The degree of loss especially relative to the peptide was unexpected but conceivably could be a consequence of steric hindrance from the HSA, which may restrict the peptide from binding to the channel pore. In an attempt to reduce potential steric effects of the fusion partner, we modified the amino acid composition of the linker by adjusting its structure and length. The linkers tested in HSA fusions included the flexible glycine serine repeats (G_4S) and the structured alanine proline (AP) repeats (30–34), ranging in length from 24 to 64 amino acids. KV261-HSA fusions utilizing AP linkers were 5–10-fold more potent than those with G_4S linkers in blocking T cell activation (Fig. 2*c*). Increasing the AP and G_4S repeat linker length from 24 to 44 amino acids enhanced Kv1.3 potency, but elongation to 64 amino acids did not result in further potency improvement. The optimal linker was found to be $AS(AP)_{20}GS$, and the corresponding fusion protein KV261-HSA-34 blocked Kv1.3 currents with an IC_{50} of 1.3 ± 0.37 nM and exhibited selectivity of >100-fold over all Kv1.x subfamily members and hERG (Fig. 2*d*), with the exception of Kv1.6, which was inhibited by KV261-HSA-34 with an IC_{50} of 9.9 ± 0.65 nM (Fig. 2*d*). KV261-HSA-34 was efficacious in inhibiting IL-2 production from anti-CD3- and anti-CD28-stimulated human $CD4^+$ T cells with an IC_{50} of 2.2 ± 0.3 nM (Fig. 2*e*).

Amino Acid Insertion to Peptide C Terminus—The potency of HSA fusions was considerably lower than the KV261 peptide as demonstrated in the previous section, possibly due to disrup-

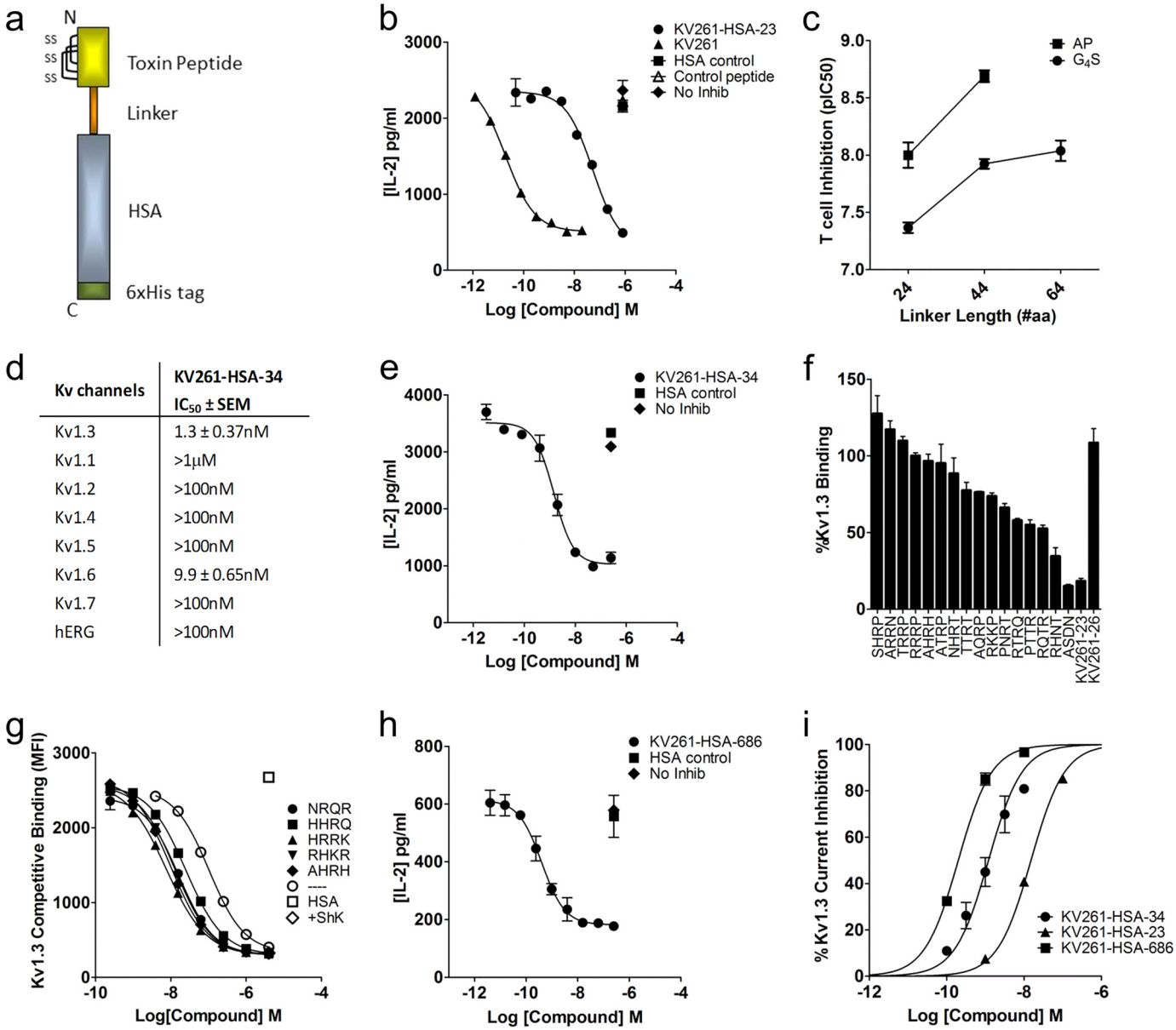

FIGURE 2. **Toxin peptide HSA fusion proteins are active and retain selectivity but require extensive engineering to optimize potency.** *a*, schematic representation of a toxin peptide-HSA fusion protein showing HSA fused off of the peptide C terminus with an intervening amino acid linker and a C-terminal His_6 purification tag. The peptide-HSA molecule is a single chain protein. *N* and *C* designate the termini. *b*, inhibition of IL-2 production from anti-CD3/anti-CD28-stimulated human $CD4^+$ T cells by KV261 (free peptide) (▲) and KV261-HSA-23 (●). *c*, increased linker length (*#aa*, number of amino acids) enhances the potency of the 261-HSA fusion constructs, and constructs with structured AP linkers (■) are more potent than constructs with G_4S (●) linkers. *d*, summary table of KV261-HSA-34 potency (IC_{50} ± S.E.) on Kv channels and hERG. Values of >100 nM or >1 μM indicate no inhibition measured up to the highest concentration tested. *e*, inhibition of IL-2 production from anti-CD3/anti-CD28-stimulated human $CD4^+$ T cells by KV261-HSA-34. *f*, C-terminal insertion variants in the $GS(G_4S)_4$-HSA fusion construct show increased binding to Kv1.3-transfected HEK cells relative to the KV261-HSA-23 (261-$GS(G_4S)_4$-HSA) parent up to the level of the KV261-HSA-26 (261-$GS(G_4S)_8$-HSA) control. *g*, C-terminal insertion variants in the $AS(AP)_{20}GS$-HSA fusion construct show improved potency over the KV261-HSA-34 without C-terminal insertion (—-) control in competitive binding. *h*, inhibition of IL-2 secretion from stimulated human $CD4^+$ T cells by the C-terminal insertion variant KV261-HSA-686. *i*, inhibition of Kv1.3 in transfected CHO cells by KV261-HSA fusions measured by manual patch clamp electrophysiology.

tion of contacts between the peptide C-terminal region and the Kv1.3 channel pore. It was hypothesized that extending the KV261 peptide C terminus in HSA fusions might restore binding affinity. KV261-HSA-23 was modified by inserting 4 amino acids between the peptide C terminus and the $GS(G_4S)_4$ linker using 12 amino acids (Gln, Arg, Pro, His, Lys, Thr, Asn, Ser, Glu, Gly, Ala, and Asp) at each position in combination. The ratio for each amino acid residue was 1, except that Arg was 1.5, and Ser was 0.5, and the resulting theoretical number of all possible variants was 12^4 (20,736). Crude supernatants of transfected cells expressing the different variants were screened for improved Kv1.3 binding affinity or enhanced inhibitory potency on Kv1.3-mediated thallium flux compared with the parent KV261-HSA-23. Lead candidates were purified and their activities relative to KV261-HSA-23, and the more potent KV261-HSA-26 (261-$GS(G_4S)_8$-HSA) was confirmed in direct Kv1.3 binding assays (Fig. 2*f*). Hits from this library were shown to contain inserts enriched for basic (Arg, His, and Lys), acidic

TABLE 3

Summary of KV261 and KV261 fusion proteins on Kv1.3 potency and selectivity in electrophysiology, inhibition of IL-2 secretion from stimulated human $CD4^+$ T cells and induction of inflammatory TNFα from PBMC cultures.

TNFα induction is shown as -fold induction over basal levels in untreated PBMC cultures. Compounds showing low potency or TNFα induction are highlighted.

Compound ID	Description	Kv1.3 Electrophysiology IC_{50} (nM) ±S.E. (fold loss from KV261)	Kv1.3 Electrophysiology Selectivity (Kv1.3/Kv1.1)	Inhibition T cell IL-2 IC_{50} (nM) ±S.E.	PBMC TNFα fold induction
KV261	261 peptide	0.02 ± 0.003 (1)	170	0.05 ± 0.01	0.3
KV261-Fc	261-GS$(G_4S)_4$-Fc	0.15 ± 0.011 (8)	710	3.20 ± 0.70	77.1
KV261-HSA-23	261-GS$(G_4S)_4$-HSA	14.70 ± 0.700 (774)	>1000	47.70 ± 5.10	2.6
KV261-HSA-34	261-AS$(AP)_{20}$GS-HSA	1.30 ± 0.370 (68)	>1000	2.20 ± 0.30	0.4
KV261-HSA-686	261-AHRH-AS$(AP)_{20}$GS-HSA	0.20 ± 0.009 (11)	>1000	0.30 ± 0.10	1.2

(Thr, Asn, and Gly), and non-polar (Ala and Pro) amino acids. Lead insertion sequences were then incorporated into the KV261-HSA-34 fusion to determine if the potency gain from amino acid insertion could further enhance the potency of HSA fusions utilizing the optimized linker AS$(AP)_{20}$GS. Several fusion proteins with inserted amino acids were confirmed to have 5–10-fold improvements in potency relative to KV261-HSA-34 in Kv1.3 binding assays (Fig. 2*g*). KV261-HSA-686 is derived from KV261-HSA-34 by insertion of 4 amino acids AHRH at the KV261 peptide C terminus. KV261-HSA-686 showed improved inhibitory potency on Kv1.3 currents (IC_{50} of 0.2 ± 0.009 nM) (Fig. 2*i*) and T cell activation (IC_{50} of 0.3 ± 0.1 nM) (Fig. 2*h*) compared with KV261-HSA-34.

In contrast to the findings with the bivalent Fc fusion proteins, the monovalent HSA fusions including KV261-HSA-34 and KV261-HSA-686 did not induce any detectable inflammatory cytokines from human PBMCs at concentrations up to 2 μM (Table 2). Table 3 summarizes the characterization results from engineering KV261 fusion proteins from KV261-Fc through the KV261-HSA fusions including potency, selectivity, and PBMC cytokine induction.

Pharmacokinetics and Pharmacodynamics of Fusion Proteins in Rats and Minipigs—To evaluate the *in vivo* pharmacokinetics of fusion proteins, Sprague-Dawley rats were administered with KV261-Fc (3.0 mg/Kg) or KV261-HSA-34 (2.3 mg/kg) by intravenous bolus, and blood samples were collected at different time points up to 4 days. Compound plasma levels were analyzed in ELISA- and FACS-based assays to specifically detect the intact fusion proteins, the fusion partners, or the KV261 peptide. The levels measured in each of the detection methods were similar, indicating that a high percentage of the compounds were intact fusion proteins over the time course of pharmacokinetic studies. The half-lives of KV261-Fc and KV261-HSA-34 in Sprague-Dawley rats were estimated to be about 72 and 14 h, respectively (Fig. 3, *a* and *b*).

KV261-HSA-34 was potent in blocking Kv1.3 currents in minipig T cells with an IC_{50} of 1.6 ± 0.29 nM (Fig. 3*c*). T cell cytokine IL-17A was induced in human and minipig blood by thapsigargin treatment and was inhibited by KV261-HSA-34 with an IC_{50} of 0.5 nM, $n = 1$ in human, and 0.5 nM, $n = 1$ in minipig blood (Fig. 3, *d* and *e*). These findings suggest that minipigs could be an appropriate species for validating Kv1.3 function in animal models (11). The pharmacokinetics of KV261-HSA-34 was tested in Yucatan minipigs after intravenous administration of the fusion protein at 2.3 mg/kg. The plasma half-life of KV261-HSA-34 was ~5–7 days, the clearance rate was 0.08 – 0.01 ml/min/kg, and the volume of distribution was 90 – 120 ml/kg (Fig. 3*f*). Kv1.3 target engagement was assessed in the same animals by measuring the inhibition of thapsigargin-induced IL-17A production from whole blood samples *ex vivo* (Fig. 3*g*). Base-line levels of thapsigargin-induced IL-17A in whole blood were established with blood samples from minipigs before KV261-HSA-34 administration as well as from the control animal, which did not receive the compound. Thapsigargin-induced IL-17A production in blood was significantly reduced starting from 1 min post-administration of KV261-HSA-34 and remained suppressed on day 14 when KV261-HSA-34 plasma levels were >10 nM. The levels of thapsigargin-induced IL-17A gradually recovered from day 36 and were back to pre-dose levels by day 54.

The Effect of KV261-HSA-34 on DTH in Minipigs—The effect of KV261-HSA-34 on T cell-mediated DTH response was evaluated in Yucatan minipigs immunized and challenged with KLH. KV261-HSA-34 had no effect on KLH-mediated DTH response in minipigs, determined by the extent of induration, challenge site inflammation scores, or levels of KLH-specific antibody titers in serum compared with the vehicle control group (Fig. 4, *a--c*). In contrast, the positive control animals dosed with cyclosporine A showed significant decreases in all three measures. KV261-HSA-34, however, reduced cell numbers in the draining lymph nodes relative to the vehicle control group. The effect was similar to that seen in the cyclosporine A-treated group, where cell numbers were reduced to levels comparable with those in the unimmunized control animals (Fig. 4*d*). Inhibition of thapsigargin-induced IL-17A production from whole blood samples confirmed that target engagement was achieved in KV261-HSA-34 and cyclosporine A-treated animals (data not shown).

DISCUSSION

In the present studies we show that the activity of the scorpion peptides, OdK2 and OsK1, can be maintained when fused to large half-life extension proteins such as human Fc or HSA. Different components of the resulting fusion proteins, including the peptide, the linker, and the fusion partner, all contribute

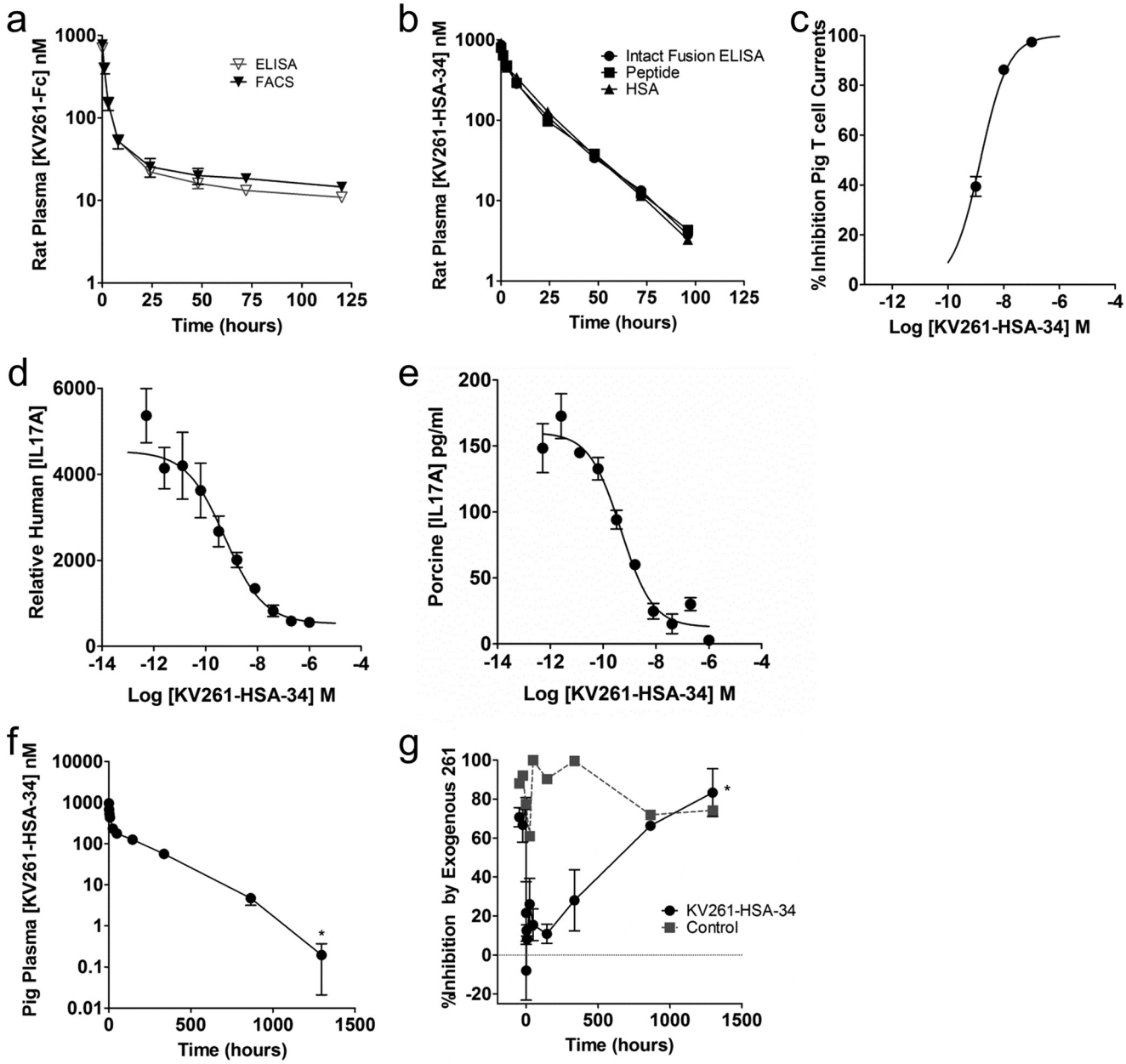

FIGURE 3. **Pharmacokinetics and pharmacodynamics of KV261-fusions in rats and mini-pigs.** *a*, KV261-Fc plasma levels in Sprague-Dawley rats were measured by detecting the Fc fragment (▽) and the intact fusion protein (▼). Rats ($n = 3$) were intravenously administered with KV261-Fc at 3.0 mg/kg, and KV261-Fc *in vivo* half-life was determined to be ~72 h. *b*, KV261-HSA-34 plasma levels in Sprague-Dawley rats were measured by detecting intact fusion protein (●), the peptide (■), and the HSA fusion partner (▲). Rats were intravenously administered with 2.3 mg/kg of KV261-HSA-34. *c*, inhibition of Kv1.3 currents in minipig $CD4^+$ T cells by KV261-HSA-34 measured using manual whole cell patch clamp electrophysiology. *d*, inhibition of IL-17A production from thapsigargin-stimulated human whole blood *in vitro* by KV261-HSA-34. *e*, inhibition of IL-17A production from thapsigargin-stimulated minipig whole blood *in vitro* by KV261-HSA-34. *f*, KV261-HSA-34 plasma levels in Yucatan minipigs after intravenous administration of KV261-HSA-34 at 2.3 mg/kg. Results shown are the average ± S.E. from four animals measured through day 36 and 2 animals at day 54. Half-life was calculated to be 5–7 days. *g*, pharmacodynamics of KV261-HSA-34 in minipigs was assessed in the same animals used in the pharmacokinetic study described in *f*. Blood samples collected from KV261-HSA-34 intravenously dosed animals (●) and a non-dosed control animal (■) were stimulated with thapsigargin *ex vivo*, and levels of induced IL-17A in whole blood were measured. The levels of thapsigargin-induced IL-17A correlate with Kv1.3 activity in blood. Thapsigargin-induced IL-17A was minimal in blood collected from KV261-HSA-34-injected minipigs from 1 min to 14 days post-administration. A gradual recovery of IL-17A was observed on days 36–54, correlating with the clearance of KV261-HSA-34 from circulation.

to the properties of the assembled molecules. The rank order of fusion proteins in potency and selectivity is similar to that of the peptides, suggesting, not surprisingly, that the potency and selectivity of a fusion molecule are strongly influenced by the peptide. Furthermore, we show that dramatic improvements in Kv1.3 selectivity can be achieved through minor changes to the venom peptide primary sequence. Valency appears to influence potency and may explain some of the potency loss in converting from bivalent Fc to monovalent HSA fusions. It is not entirely clear, but the degree of potency loss may implicate other contributing factors, such as steric hindrance from the fusion partner, which restricts the peptide from binding to the channel pore. Our results show that most of the potency loss can be rescued by engineering the linker and the peptide C terminus.

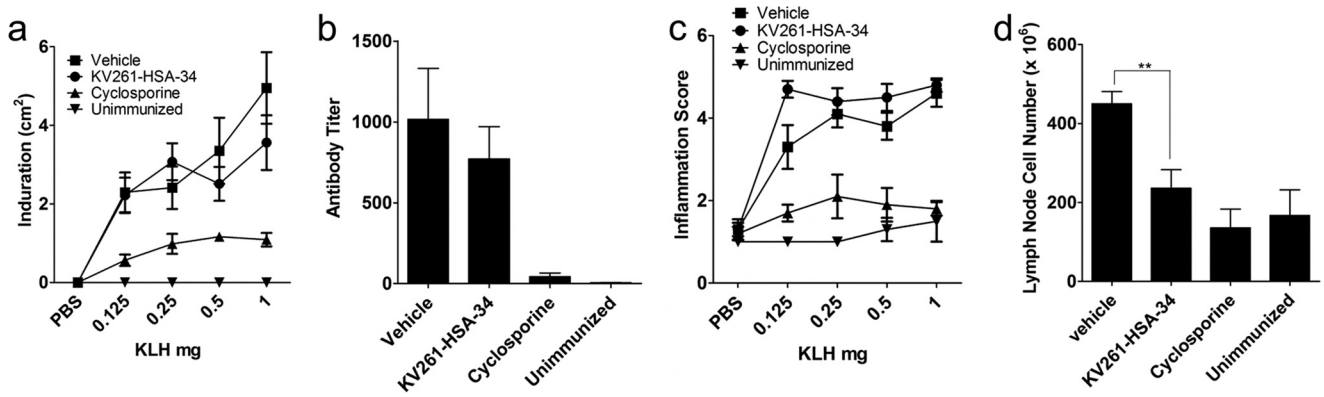

FIGURE 4. **KV261-HSA-34 did not show significant reduction of DTH response in minipigs.** Yucatan minipigs were immunized with 5 mg of KLH/incomplete Freund's adjuvant per animal on day 0 and challenged 7 days later with KLH in dorsal skin at a range of doses. Immunized Yucatan minipigs were dosed with KV261-HSA-34, cyclosporine A, and vehicle control ($n = 6$ per treatment group) as described under "Experimental Procedures." Unimmunized pigs ($n = 2$) were used as negative controls. Results were from readouts measured in duplicate and an average of $n = 6$ per treatment group ± S.E. and an average $n = 2$ ± S.E. for the unimmunized controls. *a*, no significant effect of KV261-HSA-34 (●) on induration relative to the vehicle control (■) 48 h after KLH challenge in the DTH model. Cyclosporine A (▲) reduced induration levels. KLH dorsal skin challenge doses are shown along the *x* axis. *b*, no significant reduction in anti KLH antibody titers in the KV261-HSA-34 treatment group relative to the vehicle control. Cyclosporine A reduced antibody titers down near the level of the unimmunized controls. *c*, no significant effect of KV261-HSA-34 (●) on challenge site inflammation relative to the vehicle control (■). Inflammation scores were determined by pathologist scoring of challenge site biopsy sections stained with H&E. Cyclosporine A (▲) reduced inflammation scores. KLH dorsal skin challenge doses are shown along the *x-axis*. *d*, KV261-HSA-34 and cyclosporine A significantly (**, $p = 0.0034$) reduced draining lymph node cell numbers relative to the vehicle control after KLH challenge in the DTH model.

Consistent with the steric hindrance hypothesis, we found that extended and structured linkers, such as the 20× Ala-Pro repeats, are preferred for better potency. We speculate that these linkers may create space between the peptide and the fusion moiety to reduce negative steric influences. Further gains in potency could be achieved by insertion of amino acid residues between the peptide C terminus and the linker. It is possible that these amino acids enhance the interactions of the peptide C terminus with the Kv1.3 pore loop, but other effects on the linker structure cannot be discounted. We also found some evidence that the fusion moiety may have a modest influence on target selectivity, as suggested by the slightly improved selectivity of OdK2-Fc fusion compared with the peptide.

An unexpected finding of our study was that bivalent peptide-Fc, but not peptides or monovalent HSA fusions, induced inflammatory cytokine release from human PBMCs (Table 1). The mechanism for this effect is still unclear. However, given that inflammatory cytokine release from human PBMCs was only observed with Fc fusions, it seems plausible that the underlying mechanism may involve Kv1.3 channel clustering, cell cross-linking, and effector functions resulting in undesirable immune cell activation. KV261-HSA-34, a fusion protein comprising a blocking peptide fused to human serum albumin through an intervening $AS(AP)_{20}GS$ linker, combined desirable potency, selectivity, and *in vivo* half-life in a molecule that is devoid of inflammatory cytokine-inducing issues. This molecule exhibits low nanomolar potency in blocking Kv1.3 currents and human T cell activation (Fig. 2, *d*, *e*, and *i*). It shows substantial selectivity against hERG and most of the Kv1.x subfamily members, with the exception of Kv1.6, and demonstrated long *in vivo* half-life in rats and minipigs (Fig. 3, *b* and *f*). KV261-HSA-34, therefore, is a unique biologic tool that could be used to further investigate the biology of Kv1.3 and could be considered for development for the treatment of autoimmune diseases in humans.

To explore the *in vivo* activity of a selective Kv1.3 inhibitor, we evaluated KV261-HSA-34 in a minipig DTH model. Yucatan minipigs were selected as an appropriate preclinical species to investigate *in vivo* activity of KV261-HSA-34 based on a previous published report (11). We confirmed that KV261-HSA-34 was a potent inhibitor of minipig Kv1.3 and effective in blocking thapsigargin-induced IL-17A in minipig blood (Fig. 3, *c* and *e*). Despite clear evidence of target engagement by KV261-HSA-34 at the doses used in the minipig DTH model, there were no significant effects on DTH response at the antigen challenge sites or the generation of anti-KLH antibody in response to immunization (Fig. 4, *a--c*). These findings were somewhat unexpected given previous findings of efficacy with Kv1.3 inhibitors in minipig DTH models (11). It is possible that the lack of efficacy in this model is related to limited tissue distribution of KV261-HSA-34. It is also possible that the acute and stringent nature of the minipig DTH model is more suited to the assessment of strong effects from immune-suppressants, such as cyclosporine A, rather than from more immune-modulatory effects through inhibiting Kv1.3. Consistent with a modest immune modulatory effect from Kv1.3 inhibition, KV261-HSA-34 reduced cellularity of the draining lymph nodes down to the level of the un-immunized controls (Fig. 4*d*). However, it is also conceivable that our findings with a highly selective Kv1.3 inhibitor might indicate that Kv1.3 does not play an important role in immune cell regulation *in vivo*. Further studies in relevant preclinical models are warranted.

Beyond the potential applications of Kv1.3 inhibitors in the treatment of autoimmune disease and inflammation, our results illustrate the feasibility of generating subtype-selective ion channel inhibitors through engineering of venom-derived peptides. The use of engineered venom-derived peptides may represent an important complimentary or alternative approach to small molecules for targeting therapeutically relevant but under-exploited ion channels.

REFERENCES

1. Overington, J. P., Al-Lazikani, B., and Hopkins, A. L. (2006) How many drug targets are there? *Nat. Rev. Drug Discov.* **5,** 993–996
2. Ragsdale, D. S., McPhee, J. C., Scheuer, T., and Catterall, W. A. (1996) Common molecular determinants of local anesthetic, antiarrhythmic, and anticonvulsant block of voltage-gated Na^+ channels. *Proc. Natl. Acad. Sci. U.S.A.* **93,** 9270–9275
3. Doggrell, S. A. (2004) Intrathecal ziconotide for refractory pain. *Expert. Opin. Investig. Drugs* **13,** 875–877
4. King, G. F. (2011) Venoms as a platform for human drugs: translating toxins into therapeutics. *Expert Opin. Biol. Ther.* **11,** 1469–1484
5. Chi, V., Pennington, M. W., Norton, R. S., Tarcha, E. J., Londono, L. M., Sims-Fahey, B., Upadhyay, S. K., Lakey, J. T., Iadonato, S., Wulff, H., Beeton, C., and Chandy, K. G. (2012) Development of a sea anemone toxin as an immunomodulator for therapy of autoimmune diseases. *Toxicon* **59,** 529–546
6. Klint, J. K., Senff, S., Rupasinghe, D. B., Er, S. Y., Herzig, V., Nicholson, G. M., and King, G. F. (2012) Spider-venom peptides that target voltage-gated sodium channels: pharmacological tools and potential therapeutic leads. *Toxicon* **60,** 478–491
7. Vetter, I., and Lewis, R. J. (2012) Therapeutic potential of cone snail venom peptides (conopeptides). *Curr. Top. Med. Chem.* **12,** 1546–1552
8. Desir, G. V. (2005) Kv1.3 potassium channel blockade as an approach to insulin resistance. *Expert Opin Ther. Targets* **9,** 571–579
9. Beeton, C., Wulff, H., Barbaria, J., Clot-Faybesse, O., Pennington, M., Bernard, D., Cahalan, M. D., Chandy, K. G., and Béraud, E. (2001) Selective blockade of T lymphocyte K^+ channels ameliorates experimental autoimmune encephalomyelitis, a model for multiple sclerosis. *Proc. Natl. Acad. Sci. U.S.A.* **98,** 13942–13947
10. Beeton, C., Pennington, M. W., Wulff, H., Singh, S., Nugent, D., Crossley, G., Khaytin, I., Calabresi, P. A., Chen, C. Y., Gutman, G. A., and Chandy, K. G. (2005) Targeting effector memory T cells with a selective peptide inhibitor of Kv1.3 channels for therapy of autoimmune diseases. *Mol. Pharmacol.* **67,** 1369–1381
11. Koo, G. C., Blake, J. T., Talento, A., Nguyen, M., Lin, S., Sirotina, A., Shah, K., Mulvany, K., Hora, D., Jr., Cunningham, P., Wunderler, D. L., McManus, O. B., Slaughter, R., Bugianesi, R., Felix, J., Garcia, M., Williamson, J., Kaczorowski, G., Sigal, N. H., Springer, M. S., and Feeney, W. (1997) Blockade of the voltage-gated potassium channel Kv1.3 inhibits immune responses *in vivo*. *J. Immunol.* **158,** 5120–5128
12. Beeton, C., Wulff, H., Standifer, N. E., Azam, P., Mullen, K. M., Pennington, M. W., Kolski-Andreaco, A., Wei, E., Grino, A., Counts, D. R., Wang, P. H., LeeHealey, C. J., S Andrews, B., Sankaranarayanan, A., Homerick, D., Roeck, W. W., Tehranzadeh, J., Stanhope, K. L., Zimin, P., Havel, P. J., Griffey, S., Knaus, H. G., Nepom, G. T., Gutman, G. A., Calabresi, P. A., and Chandy, K. G. (2006) Kv1.3 channels are a therapeutic target for T cell-mediated autoimmune diseases. *Proc. Natl. Acad. Sci. U.S.A.* **103,** 17414–17419
13. Rus, H., Pardo, C. A., Hu, L., Darrah, E., Cudrici, C., Niculescu, T., Niculescu, F., Mullen, K. M., Allie, R., Guo, L., Wulff, H., Beeton, C., Judge, S. I., Kerr, D. A., Knaus, H. G., Chandy, K. G., and Calabresi, P. A. (2005) The voltage-gated potassium channel Kv1.3 is highly expressed on inflammatory infiltrates in multiple sclerosis brain. *Proc. Natl. Acad. Sci. U.S.A.* **102,** 11094–11099
14. Schmitz, A., Sankaranarayanan, A., Azam, P., Schmidt-Lassen, K., Homerick, D., Hänsel, W., and Wulff, H. (2005) Design of PAP-1, a selective small molecule Kv1.3 blocker, for the suppression of effector memory T cells in autoimmune diseases. *Mol. Pharmacol.* **68,** 1254–1270
15. Tarcha, E. J., Chi, V., Muñoz-Elías, E. J., Bailey, D., Londono, L. M., Upadhyay, S. K., Norton, K., Banks, A., Tjong, I., Nguyen, H., Hu, X., Ruppert, G. W., Boley, S. E., Slauter, R., Sams, J., Knapp, B., Kentala, D., Hansen, Z., Pennington, M. W., Beeton, C., Chandy, K. G., and Iadonato, S. P. (2012) Durable pharmacological responses from the peptide ShK-186, a specific Kv1.3 channel inhibitor that suppresses T cell mediators of autoimmune disease. *J. Pharmacol. Exp. Ther.* **342,** 642–653
16. Matheu, M. P., Beeton, C., Garcia, A., Chi, V., Rangaraju, S., Safrina, O., Monaghan, K., Uemura, M. I., Li, D., Pal, S., de la Maza, L. M., Monuki, E., Flügel, A., Pennington, M. W., Parker, I., Chandy, K. G., and Cahalan, M. D. (2008) Imaging of effector memory T cells during a delayed-type hypersensitivity reaction and suppression by Kv1.3 channel block. *Immunity* **29,** 602–614
17. Beeton, C., Barbaria, J., Giraud, P., Devaux, J., Benoliel, A. M., Gola, M., Sabatier, J. M., Bérnard, D., Crest, M., and Béraud, E. (2001) Selective blocking of voltage-gated K^+ channels improves experimental autoimmune encephalomyelitis and inhibits T cell activation. *J. Immunol.* **166,** 936–944
18. Gilhar, A., Bergman, R., Assay, B., Ullmann, Y., and Etzioni, A. (2011) The beneficial effect of blocking Kv1.3 in the psoriasiform SCID mouse model. *J. Invest. Dermatol.* **131,** 118–124
19. Mouhat, S., Visan, V., Ananthakrishnan, S., Wulff, H., Andreotti, N., Grissmer, S., Darbon, H., De Waard, M., and Sabatier, J. M. (2005) K+ channel types targeted by synthetic OSK1, a toxin from Orthochirus scrobiculosus scorpion venom. *Biochem. J.* **385,** 95–104
20. Abdel-Mottaleb, Y., Vandendriessche, T., Clynen, E., Landuyt, B., Jalali, A., Vatanpour, H., Schoofs, L., and Tytgat, J. (2008) OdK2, a Kv1.3 channel-selective toxin from the venom of the Iranian scorpion *Odontobuthus doriae*. *Toxicon* **51,** 1424–1430
21. Gross, A., Abramson, T., and MacKinnon, R. (1994) Transfer of the scorpion toxin receptor to an insensitive potassium channel. *Neuron* **13,** 961–966
22. Evans, G. A. (2003) *Method for the complete chemical synthesis and assembly of genes and genomes*. Publication U.S. 6521427
23. Evans, G. (2003) *Method for assembly of a polynucleotide encoding a target polypeptide*. Publication US 6670127
24. Triggle, D. J., Gopalakrishnan, M., Rampe, D., and Zheng, W. (2006) *Voltage-gated Ion Channels as Drug Targets*, p. 219, Wiley-VCH, Weinheim, Germany
25. MacLeod, H., Goodwin, D. G., Damphousse, C., Lonie, E., Xu, X., Collins, M., and Nickerson-Nutter, C. L. (eds) (2010) The DTH effector response and IL-2 are unaffected by cyclosporine A in autoimmune B6D2F1 mice. *Cell. Immunol.* **266,** 14–23
26. Warnecke, G., Avsar, M., Steinkamp, T., Reinhard, R., Niedermeyer, J., Simon, A. R., Haverich, A., and Strüber, M. (2005) Tacrolimus versus cyclosporine induction therapy in pulmonary transplantation in miniature swine. *Eur. J. Cardiothorac. Surg.* **28,** 454–460
27. Ge, X. Y., Yu, G. Y., Cai, Z. G., and Mao, C. (2006) Long-term survival of an allografted submandibular gland in a miniature swine model given immunosuppressant drugs. *Br. J. Oral Maxillofac. Surg.* **44,** 146–151
28. Cahalan, M. D., and Chandy, K. G. (2009) The functional network of ion channels in T lymphocytes. *Immunol. Rev.* **231,** 59–87
29. Lin, C. S., Boltz, R. C., Blake, J. T., Nguyen, M., Talento, A., Fischer, P. A., Springer, M. S., Sigal, N. H., Slaughter, R. S., and Garcia, M. L. (1993) Voltage-gated potassium channels regulate calcium-dependent pathways involved in human T lymphocyte activation. *J. Exp. Med.* **177,** 637–645
30. Turner, S. L., Russell, G. C., Williamson, M. P., and Guest, J. R. (1993) Restructuring an interdomain linker in the dihydrolipoamide acetyltransferase component of the pyruvate dehydrogenase complex of *Escherichia coli*. *Protein Eng* **6,** 101–108
31. McCormick, A. L., Thomas, M. S., and Heath, A. W. (2001) Immunization with an interferon-γ-gp120 fusion protein induces enhanced immune responses to human immunodeficiency virus gp120. *J. Infect. Dis.* **184,** 1423–1430
32. Bhandari, D. G., Levine, B. A., Trayer, I. P., and Yeadon, M. E. (1986) ^1H NMR study of mobility and conformational constraints within the proline-rich N-terminal of the LC1 alkali light chain of skeletal myosin. Correlation with similar segments in other protein systems. *Eur. J. Biochem.* **160,** 349–356
33. Evans, J. S., Levine, B. A., Trayer, I. P., Dorman, C. J., and Higgins, C. F. (1986) Sequence-imposed structural constraints in the TonB protein of *E. coli*. *FEBS Lett.* **208,** 211–216
34. Packman, L. C., Hale, G., and Perham, R. N. (1984) Repeating functional domains in the pyruvate dehydrogenase multienzyme complex of *Escherichia coli*. *EMBO J.* **3,** 1315–1319